Star Formation in Proto Dwarf Galaxies

A. Noriega-Crespo* *Canadian Institute for Theoretical Astrophysics*
P. Bodenheimer and D. N. C. Lin *Lick Observatory, University of California*
G. Tenorio-Tagle *Max-Planck-Institut für Astrophysik*
* Present address: *University of Washington, Seattle.*

Abstract

The effects of the onset of star formation on the residual gas in primordial low-mass Local-Group dwarf spheroidal galaxies is studied by a series of hydrodynamical simulations. The models have concentrated on the effect of photoionization. The results indicate that photoionization in the presence of a moderate gas density gradient can eject most of the residual gas on a time scale of a few 10^7 years. High central gas density combined with inefficient star formation, however, may prevent mass ejection. The effect of supernova explosions is discussed briefly.

Introduction:

The age spread observed in several dwarf stellar systems, based on the color and [Fe/H] of individual stars within the system (see below), suggests that a large fraction of their primordial gas was retained, despite the energy release by their earliest generation of massive stars.

A significant variation in [Fe/H] is found from the observed spectroscopic data of individual stars in the dwarf elliptical galaxies Draco and Ursa Minor (Zinn 1978; Kinman *et al.* 1981). The broad red giant branch photometrically observed in the dwarf galaxies Fornax (Buonanno *et al.* 1985), NGC 147 (Mould *et al.* 1983), NGC 205 (Mould *et al.* 1984), and Draco (Carney & Seitzer 1986) also indicates a spread in metallicity (see review by Aaronson 1986).

That some fraction of the gas remains inside the system is essential for the formation of the "next generation" of stars, and for the self-enrichment by the by-products of the first supernova (SN) explosions.

In this communication we present some numerical hydrodynamical simulations of the evolution of the residual gas for several dwarf models. We first consider just the effects of photoionization. This process seems to be an effective mechanism to remove gas from proto-globular clusters and to reduce, therefore, further self-enrichment (see *e.g.* Tenorio-Tagle *et al.* 1986). Some of these models have been recently published (see Noriega-Crespo *et al.* 1989). We present also some preliminary results of a more 'realistic' set of models, which include both the HII region and supernova phases (HII-SN), and the presence of an external medium.

Photoionization:

The photoionization models considered galactic systems in the size range 0.3 to 1.0 kpc and in the mass range 10^5 to 10^7 $M_\odot$ (see table). The HII-SN models have focused on the larger systems with a tidal radius of 1 kpc and a mass of $\gtrsim 10^7$ $M_\odot$. These models included the presence of a warm, neutral, low density external medium that extends from 1 to 3 kpc.

The main assumptions include: (i) a spherically symmetric gravitational potential (time independent) for the galaxy, given by a King model (King 1966), (ii) a low metal abundance in most cases, (iii) an initial mass function similar to that in the solar neighborhood, (iv) an ionizing source located at the center of the galaxy (later on the supernova energy source), and (v) a mass in the gaseous component which is a substantial fraction of the total mass. The dynamics are examined for the relevant ranges of mass in gas, stars, matter and of galactic radius, metallicity, ionizing flux, and initial gas density distribution. The HII-SN models will examine also the supernova energy and the concentration of the gravitational potential.

Figure 1.

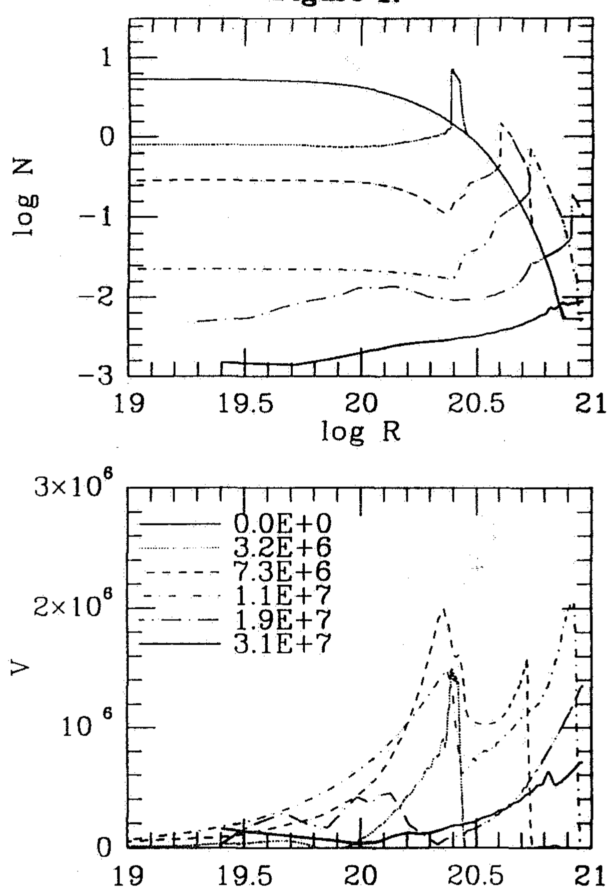

The results indicate that the effects of photoionization in the presence of a moderate gas density gradient can easily eject the gas on a time scale of a few times 10^7 years. However, with sufficiently high central gas density combined with inefficient star formation, the effect of the ionizing flux may be localized to prevent mass ejection.

Model Parameters

(1) Model	(2) M_{DM}	(3) c	(4) R_t	(5) M_G	(6) ρ	(7) Z	(8) f	(9) F_*	(10) t_*	(11) Outflow
I.1	5.5	3	0.3	5.5	s	-2	0.010	49.0	1	E
I.2	5.5	3	0.3	5.5	s	-2	0.030	49.3	1	E
I.3	5.5	3	0.3	5.5	s	-2	0.140	50.0	1	E
I.4	5.5	3	0.3	5.5	u	-2	0.074	49.7	1	R
I.5	5.5	3	0.3	5.5	u	-2	0.140	50.0	1	R
I.6	5.5	3	0.3	5.5	u	-2	0.300	49.3	10	R
I.7	5.5	6	0.3	5.5	u	-2	0.140	50.0	1	R
II.1	6.0	3	0.3	6.0	s	-2	0.010	49.3	1	R
II.2	6.0	3	0.3	6.0	s	-2	0.050	50.0	1	M
II.3	6.0	3	0.3	6.0	s	-2	0.330	51.0	1	E
II.4	6.0	3	0.3	6.0	s	-2	0.500	50.0	10	E
II.5	6.0	6	0.3	6.0	s	-2	0.050	50.0	1	E
III.1	7.0	3	0.3	6.0	s	-2	0.010	50.0	1	R
III.2	7.0	3	0.3	6.0	s	-2	0.080	51.0	1	E
III.3	7.0	3	0.3	6.0	s	-2	0.080	50.0	10	E
III.4	7.0	3	0.3	5.5	s	-2	0.010	50.0	1	E
III.5	7.0	3	0.3	5.5	s	-2	0.001	49.0	1	R
IV.1	6.0	5	1.0	5.5	2.5	-2	0.130	50.3	1	E
IV.2	6.0	5	1.0	5.5	3.0	-2	0.130	50.3	1	M
IV.3	6.0	5	1.0	5.5	3.5	-2	0.130	50.3	1	R
V.1	7.0	5	1.0	6.5	3.8	-2	0.015	50.3	1	E
V.2	7.0	5	1.0	6.5	3.95	-2	0.015	50.3	1	R
V.3	7.0	5	1.0	6.5	3.95	-2	0.130	51.3	1	R
V.4	7.0	5	1.0	6.5	3.95	-2	0.130	50.3	10	E
V.5	7.0	5	1.0	6.5	3.80	0	0.015	50.3	1	R
V.6	7.0	5	1.0	6.5	3.80	0	0.130	51.3	1	R

Column (1) lists the model number. Columns (2) and (5) list the logarithms of the stellar and gas mass, respectively, in units of $M_{\odot}$. Columns (3) and (4) indicate the concentration parameter c, and the tidal radius of the galaxy in kpc, respectively. In Column (6), the gas density distribution is indicated. The symbol *s* represents a gas distribution scaled to the stellar distribution. The symbol *u* represents uniform initial density. The numerical entries represent the logarithm of the equilibrium temperature in the isothermal cases. Column (7) gives the logarithm of the metal abundance, in solar units. Columns (8) and (9) represent the star formation efficiency, as defined by eqn. (1), and the logarithm of the ionizing flux in photons s^{-1}, respectively. Column (10) represents the characteristic lifetime for the ionizing flux, in units of 4×10^6 yr. Column (11) indicates the evolutionary outcome where the symbols *R*, *M*, and *E* represent gas retention, marginal mass loss, and total gas ejection, respectively.

Figure 1 shows, as an example, the evolution of the density and velocity distributions as a function of time for one of our photoionization low mass models (model I.1). The different lines correspond to different times. The model has a total mass $M_T = 3.3 \times 10^5$ $M_{\odot}$, and a similar mass in gas with a metallicity $Z=10^{-2}$ $Z_{\odot}$. The model has a very low ionizing flux, 10^{49} photons s^{-1}, equivalent to one massive star (~ 20 $M_{\odot}$). The system evolves into an ionization front preceded by a shock front (D-type), separated by a dense shell. In this case the photoionization provided with enough momentum to the gas that $\sim 90\%$ is removed in $\sim 3 \times 10^7$ years.

The effect of supernova explosions

For some models a flat density distribution seems to suppress gas mass loss driven by photoionization. In these cases (*e.g.* V.2 or V.6) the effect of SN explosions can eject all the gas. Figure 2. shows the time evolution of the gas density of a blast wave in a flat density distribution model. The parameters are those of model V.5 where there was no gas ejection by photoionization. The model includes the presence of an external medium that extends beyond the 1 kpc "optical" tidal radius up to 3 kpc.

Figure 2.

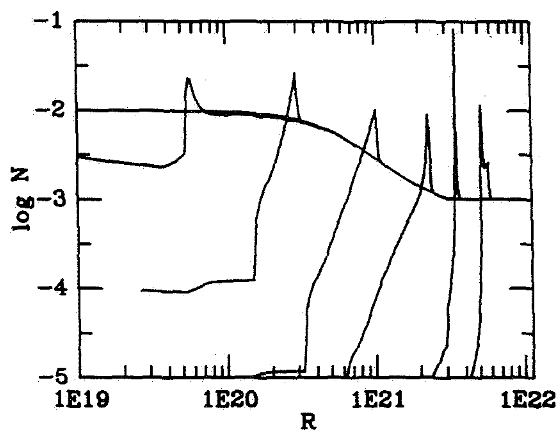

In this case the photoionization evolution was followed up to $\sim 3.2556 \times 10^6$ yrs. At this time the supernovae energy, 2×10^{52} ergs, is set at the inner boundary and the ionizing flux is turn off ($t = 0$). The different lines in Figure 2 correspond to different times. From left to right 0.0e+0, 9.4e+4, 5.4e+5, 2.9e+6, 9.2e+6 and 3.4e+7 years, respectively. The shock wave moves initially at several 10^8 cm s^{-1}, but by the last model, at 3.4×10^7 yrs, the gas is moving at $\sim 1.8 \times 10^6$ cm s^{-1}.
In this model all the gas inside the 1 kpc radius ($\sim$ %10 of the total gas mass) is ejected at $\sim 7 \times 10^6$ yrs after the explosion.

The results suggest that, given a normal initial mass function, many protodwarf galaxies may have been dispersed by the onset of star formation.

ANC thanks Laurie Feinswog for exhilarating discussions and her technical advice. ANC thanks the Connaught Fund of University of Toronto and the NSERC of Canada for their support to this project. He also thanks the Organizing Committee and the NSF under Grant AST 87-17867 for their support to participate in this meeting.

References

Aaronson, M., 1986. In: *Star-Forming Dwarf Galaxies*, p. 125. eds Kunth, D., Thuan, T. X. & Tran Thanh Van, J., éditions Frontières, Gif sur Yvette, France.

Buonanno, R., Corsi, C. E., Fusi Pecci, F., Hardy, E. & Zinn, R., 1985. *Astr. Astrophys.*, **152**, 65.

Carney, B. W. & Seitzer, P., 1986. *Astr. J.*, **92**, 23.

King, I. R., 1966. *Astr. J.*, **71**, 64.

Kinman, T. D., Kraft, R. P. & Suntzeff, N. B., 1981. In: *Physical Processes in Red Giants*, p. 71, eds Iben, I. Jr. & Renzini, A., Reidel, Dordrecht, Holland

Mould, J. R., Kristian, J. & DaCosta, G. S., 1983. *Astrophys. J.*, **270**, 471.

Mould, J. R., Kristian, J. & DaCosta, G. S., 1984. *Astrophys. J.*, **278**, 575.

Noriega-Crespo, A., Bodenheimer, P., Lin, D. N. C. & Tenorio-Tagle, G., 1989. *Mon. Not. R. astr. Soc.*, **237**, 461.

Tenorio-Tagle, G., Bodenheimer, P., Lin, D. N. C. & Noriega-Crespo, A., 1986. *Mon. Not. R. astr. Soc.*, **221**, 635.

Zinn, R., 1978. In: *Globular Clusters*, p. 191, eds Hanes, D. & Madore, B., Cambridge University Press.